Agronomy Research **19**(S1), 928–943, 2021
https://doi.org/10.15159/AR.21.023

Effect of hydrothermal carbonization and torrefaction on spent coffee grounds

E. Sermyagina[1,*], C. Mendoza[1,2] and I. Deviatkin[3]

[1]LUT University, Department of Energy Technology, PL 20, 53851 Lappeenranta, Finland
[2]Federal University of Minas Gerais, 31270-901 Belo Horizonte, MG Brazil
[3]LUT University, Department of Sustainability Science, PL 20, 53851 Lappeenranta, Finland
[*]Correspondence: ekaterina.sermyagina@lut.fi

Received: February 1st, 2021; Accepted: March 28th, 2021; Published: April 6th, 2021

Abstract. Coffee is one of the most tradable commodities worldwide with the current global consumption of over 10 billion kilograms of coffee beans annually. At the same time, a significant amount of solid residues, which are known as spent coffee grounds (SCG), is generated during instant coffee manufacturing and coffee brewing. Those residues have a high potential in various applications, yet they remain mostly unutilized. The current work presents the experimental comparison of two pretreatment technologies - hydrothermal carbonization (HTC) and torrefaction - for converting SCG into a valuable char. The results showed that low-temperature torrefaction (< 250 °C) has a negligible effect on feedstock properties due to initial pre-processing of coffee beans. However, the energy conversion efficiency of torrefaction at higher temperatures is comparable with that of HTC. The average energy yields for high-temperature torrefaction (> 250 °C) and HTC were on the level of 88%. Devolatilization and depolymerization reactions reduce oxygen and increase carbon contents during both processes: chars after torrefaction at 300 °C and HTC at 240 °C had 23–28% more carbon and 43–46% less oxygen than the feedstock. Both pretreatment methods led to a comparable increase in energy density: the highest HHV of 31.03 MJ kg^{-1} for torrefaction at 300 °C and 32.33 MJ kg^{-1} for HTC at 240 °C, which is similar to HHV of anthracite. The results showed that both processes can be effectively used to convert SCG into energy-dense char, even though HTC led to slightly higher energy densification rates.

Key words: biomass pretreatment, hydrothermal carbonization, torrefaction, spent coffee grounds.

INTRODUCTION

In recent years, various organic waste and by-products have been attracting increased attention as feedstock materials for chemicals, materials, or energy carriers. Meanwhile, the principles of the circular economy are gaining acceptance worldwide by providing a sustainable development pathway through optimized resource utilization (Chen et al., 2021). It is generally accepted that by implementing recycling and recovery operations, waste can be converted into valuable products, thus reducing the depletion of virgin resources and the amount of land required for landfills.

Coffee is one of the most widely consumed beverages globally with the total consumption of 10 Mt of coffee beans in 2020 (ICO, 2020). Instant coffee manufacturing, as well as coffee brewing, generates a large amount of solid residues - spent coffee grounds (SCG) - that mostly remain unused due to their high moisture content and the phytotoxic nature of some of its components, such as caffeine, tannins and polyphenols (Fornes et al., 2017). The economically feasible energy generation from a moist product is generally challenging and expensive, thus SCGs are often landfilled. However, landfilling of biodegradable waste results in its anaerobic decomposition and strongly contributes to climate change and groundwater pollution due to the generation of landfill gas and leachate. Moreover, the direct application of SCG in large amounts towards biochemical application can be problematic and harmful due to the components' toxicity for many life processes (Vítězová et al., 2019).

SCG are rich in polysaccharides, lignin, proteins, and fatty acids (Murthy & Naidu, 2012; Kwon et al., 2013). Various utilization pathways can be used to convert this low-value feedstock into different value-added products. Recent studies highlight a significant potential of SCG for the production of biodiesel (Haile et al., 2013; Atabani et al., 2018) and bioethanol (Choi et al., 2012), as a feedstock for adsorbents (Felber et al., 2012; Kante et al., 2012), antioxidants (Yen et al., 2005), and fertilizers (Kasongo et al., 2011; Yamane et al., 2014). Hydrothermal carbonization (HTC) and torrefaction are two distinct options to upgrade the thermochemical properties of SCG (Moustafa et al., 2017; Kim et al., 2017). These processes produce solid products with improved handling characteristics and increased energy content. Besides, additional benefits may be found for different other application of the produced chars, e.g. SCG-derived hydrochar showed beneficial properties as a substrate for anaerobic digestion (Codignole Luz et al., 2018).

During HTC, the feedstock is mixed with water and is then heated at moderate temperatures for several hours (Tamelová et al., 2019; Partridge et al., 2020; Sermyagina et al., 2020). HTC is beneficial for wet feedstock eliminating the need for its energy-intensive drying (Zhuang et al., 2019). The temperatures of HTC range between 180–250 °C, while self-generated pressure leads to the transformation of the biomass into a carbonaceous char (or hydrochar). By-products of the process include both aqueous compounds (HTC liquor) and gaseous streams (contain approx. 90% CO_2) (Funke & Ziegler, 2010; Kambo & Dutta, 2014). The HTC liquor has the potential to produce high-value chemicals (furfurals, fatty acids, etc.) and their utilization can improve the overall performance of the process (Fuente-Hernández et al., 2017).

Torrefaction is an alternative to mild pyrolysis treatment. The process takes place at temperatures of 200–300 °C under an inert atmosphere (Velebil, 2018; Urbancl et al., 2019). During this treatment, the biomass components degrade releasing condensable and non-condensable gases, while the carbon-rich solid residue (char) is obtained (Tamelová et al., 2019). Both HTC and torrefaction lead to certain structural changes in the biomass components producing the homogeneous solid material with higher grindability, hydrophobicity and energy density in comparison with feedstock (Tamelová et al., 2019).

The impact of different pretreatments on biomass properties have been actively investigated recently (Liu & Balasubramanian, 2014; Paneque et al., 2017; Nizamuddin et al., 2018; Rodriguez Correa et al., 2019). The results of the comparative investigation of HTC and torrefaction have been reported in the recent years for various wastes and

by-products (e.g. olive tree trimmings residue (Volpe et al., 2016; Duman et al., 2020), grape pomace (Pala et al., 2014), and azolla biomass (Babinszki et al., 2020). However, the comparison of these treatment processes on SCG has not yet been addressed properly. In this work, the impact of the reaction conditions during HTC and torrefaction on the energy properties of SCG was analysed. This work expands the available knowledge of the thermo-chemical properties of SCG and derived chars. The obtained information can be effectively utilized for modelling purposes and promoting more effective valorisation of this waste stream.

MATERIALS AND METHODS

Materials

SCG were obtained after brewing the finely ground dark roast *Arabica* coffee beans (Wanyama blend by Arvid Nordquist) in a drip coffee maker. SCG were dried overnight in an oven at the temperature of 105 ± 2 °C and kept in plastic bags for further processing and analysis.

HTC reactor and procedure

The experiments were carried out in a batch reactor. The stainless steel tube reactor (1 L volume, 705 8mm height, 42 mm inner diameter) had a flange connection at the top and a screw cap at the bottom (Fig. 1). Two type K thermocouples were used to monitor the internal temperature (submerged 245 mm and 645 mm from the top respectively), while an additional thermocouple was used to monitor the outer surface temperature of the reactor. The permitted deviation of the measurement was ± 1.5 °C max according to the standard DIN EN 60 584-2. The pressure inside the reactor was measured with the pressure transmitter (WIKA, model A-10, 0–40 bar gauge) with the accuracy of ± 0.5% of span. For safety purposes, a pressure relief valve was installed in the unit (setpoint pressure 40 bar, maximum temperature of 300 °C). The reactor was heated by a controllable electric resistance heating jacket and protected by a thick insulation layer and an outer steel sheet. The required temperature level inside the reactor was maintained with a PID controller by varying the heat supply to the reactor based on the signals from the lower thermocouple. Data from the temperature and pressure sensors was recorded automatically every 3 s.

In current HTC experiments, three sets of experimental conditions were used following the methodology reported elsewhere (Sermyagina et al., 2015). The temperature was set to 200 °C, 220 °C and 240 °C. The residence time was held constant at 3 h and the water-to-biomass ratio was maintained at 6:1 (30 g of dry feedstock and 180 mL of water). At the start of each experiment, the SCG sample and water were mixed, stirred manually and then loaded into the reactor. The temperature setpoint was reached in about 30 min. After the HTC treatment, the reactor was allowed to cool down naturally to room temperature. The hydrochar and liquid product were collected and separated by vacuum filtration using Büchner funnel with Whatman glass microfiber filter paper (grade GF/A). The solid product was subsequently dried overnight in the oven at the temperature of 105 ± 2 °C and kept in plastic bags for further analysis. Each test was conducted in replicates. Mass and energy yields were calculated using the average values of the results. The analysis of the liquid and gaseous products was outside the scope of the current work and thus was not performed.

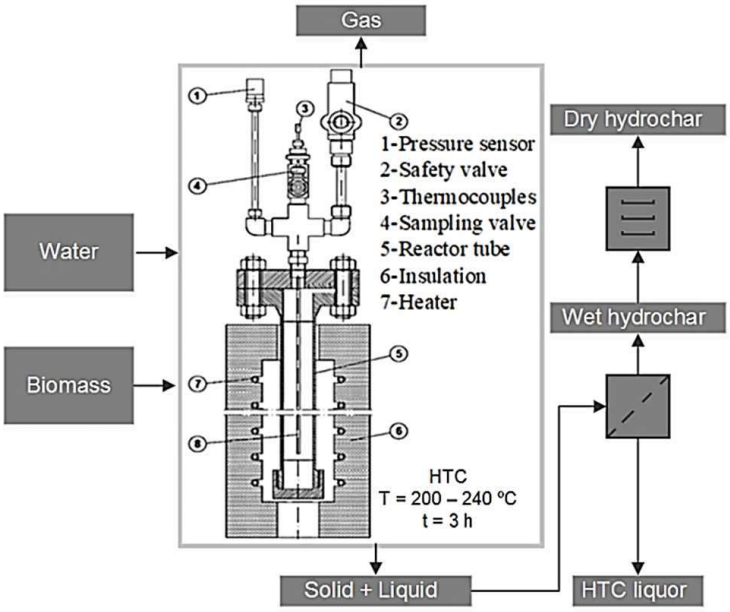

Figure 1. HTC experimental unit and experimental procedure.

Hydrochar samples were named following the process temperature as HTC-t, where t denotes the reaction temperature in °C.

Torrefaction reactor and procedur

For the torrefaction experiments, a vertical quartz tube (780 mm length, 45 mm diameter) was used with the previously described electric resistance heating jacket (Fig. 2). The feedstock was placed onto the sintered quartz glass grid in the reactor and the constant gas flow of nitrogen of 0.5 L min^{-1} was introduced and maintained by Bronkhorst mass flow controllers to obtain an inert atmosphere. The gas inlet was at the bottom part of the reactor and the outlet at the top. Two type K thermocouples were used to measure the temperature below and above the grid. The temperature inside the reactor was controlled with a PID controller by varying the heat supply on the basis of the signals from upper thermocouple. The data from temperature sensors and mass flow controllers were recorded automatically every 3 s.

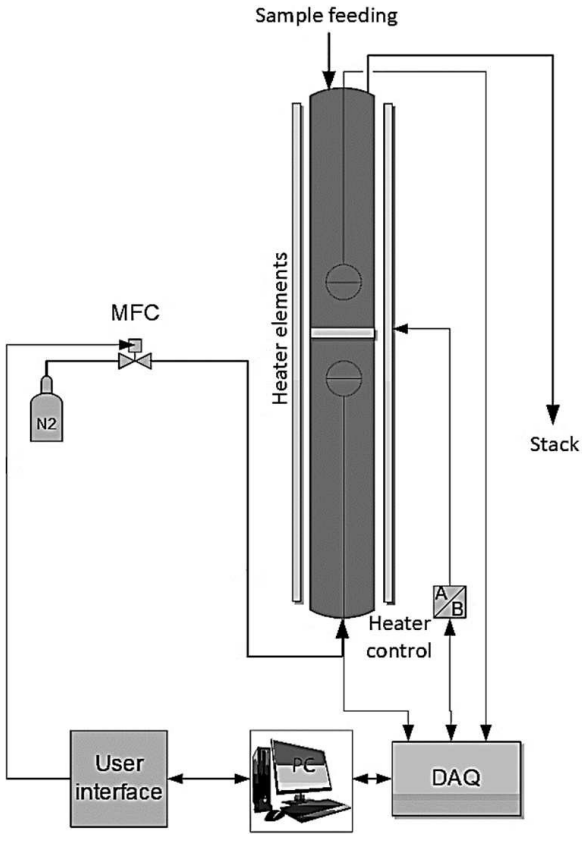

Figure 2. Bench-scale torrefaction unit.

For each torrefaction test, about 9 g of SCG were introduced into the reactor and the nitrogen was used to purge the air from the system for several minutes before the start of the heating. The temperature setpoints varied between 200 °C and 300 °C with 20 °C incremental steps. The heating rate was set on the level 10 °C min^{-1}. The residence time was held constant at 60 min. After each test, the reactor and the samples were allowed to cool down naturally to room temperature. The char was then collected and kept in plastic bags for further analysis. Torrefied char samples were named according to the process parameters as Torre-t, where t denotes the reaction temperature in °C. The analysis of the gaseous products was outside the scope of the current work.

Analytical methods

Both the SCG and the produced char samples were characterized using the standard procedures. Characterization was performed at least twice for each reaction condition, and the average value was reported.

For the proximate analysis, the samples were first dried in a laboratory oven at the temperature of 105 ± 2 °C until a constant mass was reached to determine the moisture content with the simplified oven-dry method EN 14774-2 (SFS, 2009a). The ash content was determined according to EN 14775 (SFS, 2009b) by gradually heating the sample to 550 °C and maintaining it at a constant temperature for at least 2 h. The volatile matter was measured by calculating the mass lost at the temperature of 900 ± 10 °C after 7 min without contact with air as described by EN 15148 (SFS, 2012). Fixed carbon content was determined by reducing the mass of ash and volatiles from the initial mass of the dry sample.

The elemental composition, i.e. carbon, hydrogen, nitrogen, oxygen, and sulphur, of the samples was determined following ISO 16948 (SFS, 2015) and ISO 16994 (SFS, 2016). The elemental analysis was performed with a LECO CHN628 Series Elemental Determinator coupled with a 628S Sulphur Add-On Module. Prior to the analysis, the standard samples (ethylenediaminetetraacetic acid for CHN and coal for S measurements) were first analysed to verify the experimental error within ± 1% for the elements. For CHN analysis, approximately 30 mg of oven-dry material were fed in the combustion chamber. The sulphur content was determined by using approximately 50 mg of dried material which was combusted in the sulphur module at 1,350 °C. The results are presented on a dry basis as the mean of replicates. The oxygen content was approximated as the difference between 100% and the weight percentages of the major elements and ash on a dry basis.

Thermogravimetric analysis (TGA) was performed with STA 449C thermogravimetric analyzer (Netzsch Instruments, Germany). About 10 mg of the sample were placed inside Al2O3 sample holder. The furnace was sealed and purged with high purity (99.9995 %) nitrogen flow to remove air. The sample was heated from room temperature to 900 °C at rate of 20 °C min^{-1}. Two different gas atmospheres were applied: high purity nitrogen for pyrolysis conditions and compressed air for combustion conditions. In both cases, a constant gas flow rate of 250 mL min^{-1} was maintained.

The morphology of the samples was examined by scanning electron microscopy (SEM) using a Hitachi SU3500 microscope.

The mass yield (*MY, %*) was calculated on a dry basis (d.b.) as follows:

$$MY = \frac{m_{out}}{m_{in}} \cdot 100\% \quad (1)$$

where m_{in} – the initial mass of feedstock (d.b.), g; m_{out} – the solid mass output (d.b.), g.

The energy densification ratio (*ER*) was calculated as follows:

$$ER = \frac{HHV_{prod}}{HHV_{fs}} \quad (2)$$

The energy yield (*EY, %*), was calculated as follows:

$$EY = MY \cdot ER \quad (3)$$

The higher heating values on dry basis (HHV, d.b.) of the samples were calculated with Eq. (4) from Reed & Gaur (1994):

$$HHV, d.b. = 0.3491 \cdot X_C + 1.1783 \cdot X_H + 0.1005 \cdot X_S - 0.0151 \cdot X_N - 0.1034 \cdot X_O - 0.0211 \cdot X_{AC} \quad (4)$$

where HHV in MJ kg^{-1} (d.b.); X_i - concentrations of carbon (C), hydrogen (H), oxygen (O), sulphur (S), nitrogen (N) and ash content in wt.% (d.b.). HHV_{prod} is higher heating value of the product char, MJ kg^{-1} and HHV_{fs} is higher heating value of the feedstock, MJ kg^{-1}.

RESULTS AND DISCUSSION

Mass and energy yields

The mass yield was calculated with Eq. (1). Fig. 3 presents the results of torrefaction and HTC together with the correlation curves for the char mass yield. The equations for the correlations are given between reaction temperature, T, in °C, and the mass yield values in the percentage points. The solid yield decreased with the reaction temperature for both treatment methods. In the case of torrefaction, low-degree processing (< 250 °C) had a limited effect on the SCG decomposition which can be seen from the negligible mass loss. This result could be attributed to the structural modifications that have already happened during initial roasting of coffee beans. The typical roasting temperatures are in the range of 220–240 °C, the roasting process can be compared to a low-temperature torrefaction that results limited devolatilization of SCG components. Such pre-processing explains the limited changes in the feedstock during low-degree torrefaction. At the same time, higher temperatures led to the mass loss intensification with the maximum value of 32% at 300 °C. Overall, the obtained values fit well with the polynomial correlation (R^2 = 0.999). As for the HTC tests, the reaction temperature increase led to a steady decrease in the mass yield from 81% at 200 °C to 72% at 240 °C. The HTC conditions resulted in a higher mass loss at the lower temperature limit in comparison with torrefaction. Water during this treatment acts as a catalyst and a reactant for organic compounds of the feedstock, thus making them more reactive (Román et al., 2012). Linear regression was fitted to the individual HTC runs with an R^2 value of 0.961.

The higher heating values were calculated with Eq. (4). The impact of the reaction temperature on the HHV of the products is presented in Fig. 4. The values for the coal grades are from (Donahue & Rais, 2009).The rapid increase of the heating values can be seen for the torrefied samples treated at 260 °C and higher, while low temperatures result

only in limited changes. In the case of HTC, there is a notable increase in HHV within the whole investigated range. Both treatment methods converted SCG into carbonaceous chars with heating values comparable to hard coal: 31.03 MJ kg^{-1} for Torre-300 and 32.33 MJ kg^{-1} for HTC-240. The increase in the energy content is associated with the decrease in atomic O:C and H:C ratios resulting from the decomposition reactions (Libra et al., 2011). The obtained values are reasonably similar to the previously published ones. The torrefied SCG are reported to have the HHV in the range of 26.6–29.5 MJ kg^{-1} after torrefaction at 260–275 °C and 29.8 MJ kg^{-1} at 300 °C (Zhang et al., 2018; Barbanera & Muguerza, 2020). As for the HTC, the hydrochar HHV are varying between 26.5–27.5 MJ kg^{-1} for 210–240 °C processing during 1 h (Kim et al., 2017) and between 25.5–31.2 MJ kg^{-1} after treatment during 3.5 h at 190 and 246 °C correspondingly (Massaya et al., 2021).

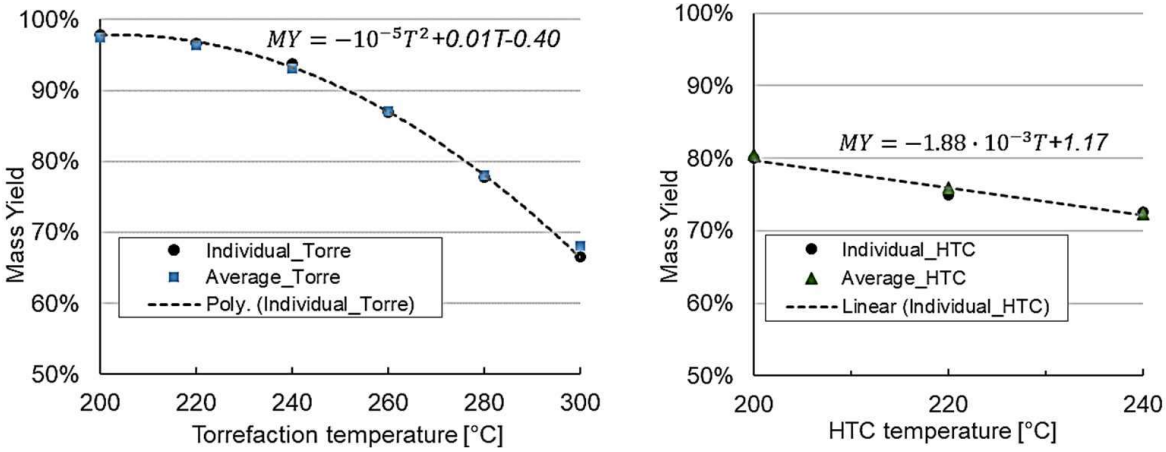

Figure 3. Mass yield of HTC experiments as a function of temperature for untreated and treated samples.

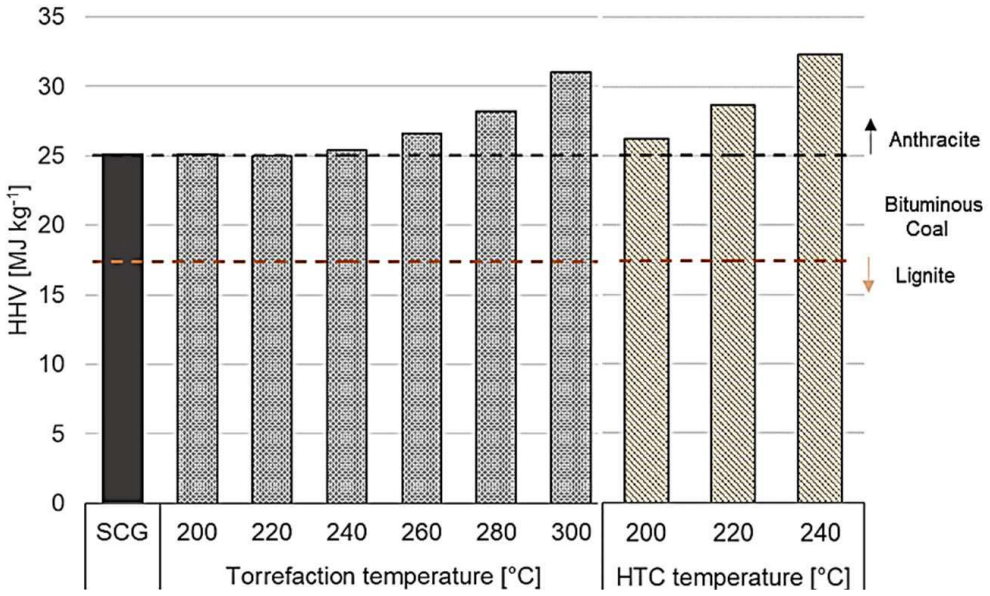

Figure 4. Higher heating values of SCG and chars produced by torrefaction and HTC.

To assess the conversion efficiency, the energy yield for each test was calculated on a dry basis with Eq. (3). This parameter indicates how much of the total energy content of the feedstock is converted to the energy content of the produced char. The energy densification ratio is another important parameter for comparing different pretreatment processes as it evaluates the upgrade in energy density from the raw feedstock. The energy densification ratio as a function of reaction temperature for torrefaction and HTC is presented in Fig. 5 along with the energy yield. The energy yield is influenced by two factors acting inversely with temperature growth: decreasing mass yield and simultaneously increasing energy densification ratio. Within HTC conditions, the mass yield of hydrochar decreased slightly with the temperature, while the increase of energy content was more pronounced. As a result, the energy yield increased along with the HTC temperature. The effect of torrefaction was notably different within the studied process parameters. At low temperatures (< 250 °C), the mass loss was small and there was no gain in the energy content. However at higher temperatures, the changes in the mass yield were more rapid, thus exceeding the gain in the heating value and resulting in a descending trend for the energy yield. Overall, the average energy yield for high-temperature torrefaction (Torre-260, Torre-280 and Torre-300) was similar to the average energy yield of the HTC tests: 88.4% and 88.1% correspondingly. Similar values were reported previously for SCG (Buratti et al., 2018; Afolabi et al., 2020; Massaya et al., 2021).

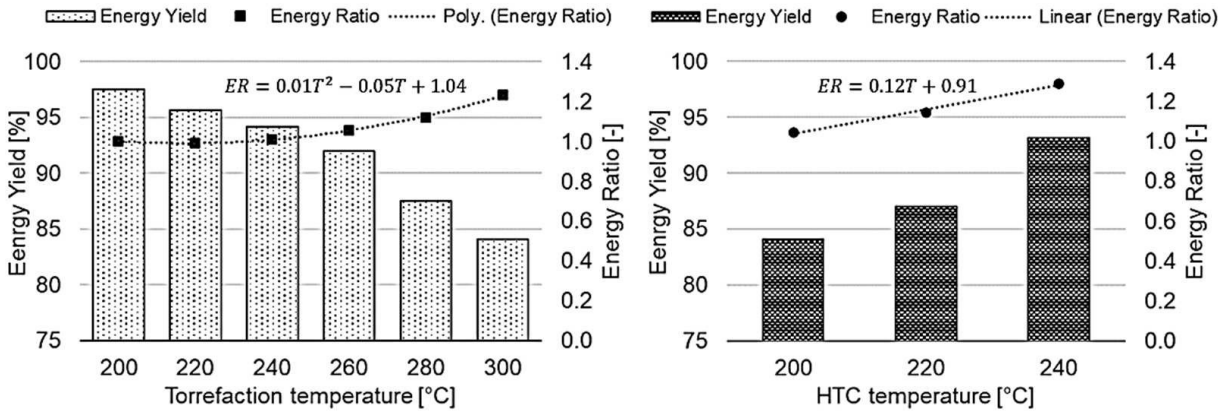

Figure 5. Energy yields and energy densification ratios of torrefaction and HTC experiments as a function of reaction temperature. Energy yield as bars is shown on left axis, while points and trendline show energy densification on right axis.

The energy densification factor ranged from 1.00 to 1.23 for torrefaction and from 1.04 to 1.29 for HTC, strongly correlating with reaction temperature. The correlations between temperatures and energy densification ratios are presented in Fig. 5. The polynomial correlation fits well the energy densification values for torrefaction tests (0.998 R^2 value). In case of HTC experiments, the linear regression model appears to fit data well by giving $R^2 = 0.987$.

Proximate and ultimate analyses

The results of proximate and ultimate analyses, along with their standard deviations, are given in Table 1. The proximate composition of the feedstock was nearly identical to the samples Torre-200 and Torre-220, meaning that low-temperature

torrefaction did not have a significant impact on the material characteristics. As the temperature increased and the SCG components started to degrade, the volatile matter decreased and the fixed carbon increased. In the case of HTC, the reaction temperature increase had a similar effect. The samples Torre-300 and HTC-240 lost 12% and 18% of volatiles, correspondingly, compared to the SCG. As a result of the volatilization of lignocellulosic components during treatments, the fixed carbon content of these samples increased 1.6 and almost 2 times in comparison with the feedstock. The tendencies are consistent with other studies (Buratti et al., 2018; Afolabi et al., 2020).

Table 1. Proximate and ultimate compositions of the samples[α]

	SCG	Torrefaction temperature [°C]						HTC temperature [°C]		
		200	220	240	260	280	300	200	220	240
	Proximate composition (wt%, db)									
VM	82.67	82.71	82.67	81.09	80.50	74.96	72.50	82.83	81.03	67.84
	(0.23)	(0.19)	(0.10)	(0.12)	(0.13)	(0.31)	(0.27)	(0.21)	(0.06)	(0.29)
AC	1.13	1.14	1.21	1.23	1.35	1.53	1.89	0.57	0.28	0.19
	(0.01)	(0.06)	(0.03)	(0.06)	(0.06)	(0.03)	(0.03)	(0.02)	(0.04)	(0.01)
FC	16.20	16.15	16.11	17.68	18.15	23.52	25.60	16.61	18.69	31.97
	(0.24)	(0.25)	(0.13)	(0.18)	(0.19)	(0.34)	(0.30)	(0.23)	(0.10)	(0.30)
	Ultimate composition (wt%, daf)									
C	55.74	55.74	56.02	56.22	58.84	62.38	68.52	57.53	61.82	71.06
	(0.05)	(0.11)	(0.01)	(0.10)	(0.23)	(0.01)	(0.12)	(0.09)	(0.03)	(0.16)
H	7.75	7.76	7.51	7.80	7.74	7.73	7.74	8.03	8.39	7.98
	(0.01)	(0.002)	(0.01)	(0.02)	(0.05)	(0.02)	(0.04)	(0.02)	(0.02)	(0.06)
N	2.36	2.34	2.38	2.39	2.53	2.77	3.13	2.18	2.30	2.93
	(0.04)	(0.01)	(0.03)	(0.04)	(0.01)	(0.02)	(0.01)	(0.08)	(0.05)	(0.02)
S	0.127	0.117	0.110	0.098	0.097	0.091	0.100	0.116	0.125	0.200
	(0.001)	(0.001)	(0.011)	(0.001)	(0.005)	(0.004)	(0.027)	(0.013)	(0.014)	(0.04)
O	32.89	32.90	32.77	32.26	29.43	25.51	18.61	31.58	27.08	17.65
	(0.11)	(0.19)	(0.09)	(0.23)	(0.36)	(0.07)	(0.24)	(0.22)	(0.16)	(0.29)

[α] Number enclosed in the parenthesis are standard deviations calculated based on error propagation from duplicate measurements.

VM – Volatile Matter; AC – Ash Content; FC – Fixed Carbon; C – Carbon; H – Hydrogen; N – Nitrogen; O – Oxygen; S – Sulphur; db – dry basis; daf – dry ash free basis.

Of particular interest is the ash content observed in the produced chars, where the opposite trends were found for torrefaction and HTC. Ash components were not affected during torrefaction and this led to the continuous increase of ash content on a weight basis in the produced chars: from 1.14 wt% for Torre-200 to 1.89 wt% for Torre-300. Ash-forming minerals were partially dissolved in the liquid phase (Broch et al., 2014), thus resulting in a notable reduction in hydrochar ash content: 50% decrease for HTC-200 and 83% for HTC-240 compared to AC of SCG. The results presented in (Afolabi et al., 2020) showed a similar decreasing tendency of ash content in hydrochar, though not as significant as in the present study. The differences can be explained by the variation in the amount of water used for the tests and affecting the extent of the dissolution: 1:10 in (Afolabi et al., 2020) versus 1:6 in the current work.

For all studied samples, carbon was the main constituent ranging 55.7 wt% for feedstock to 68.5 wt% for Torre-300 and 71.1 wt% for HTC-240. Oxygen was the second most abundant element, yet its content constantly decreased with temperature increase during both treatments. Similar tendencies were reported in the literature (Afolabi et al., 2020; Barbanera & Muguerza, 2020). There were no dramatic changes in the hydrogen content of the chars during both methods. At the same time, nitrogen content increased slowly but steadily by approximately 30% for Torre-300 and HTC-240 in comparison with the feedstock. The sulphur content of all studied samples was low. However, there was a slight decrease in the case of torrefaction and an increase in the case of HTC with temperature increase.

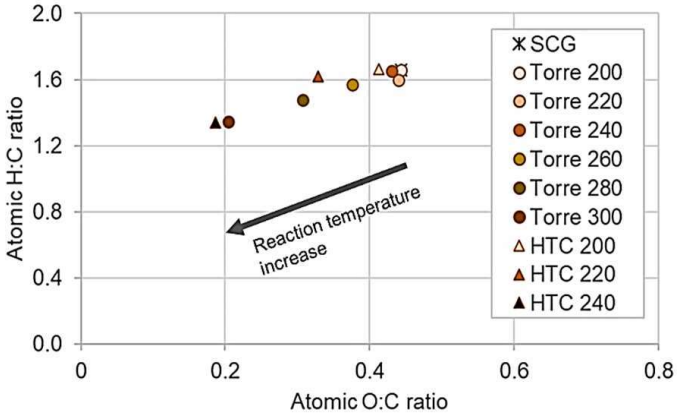

Figure 6. Van Krevelen diagram for feedstock and chars after torrefaction and HTC.

The hydrogen-to-carbon (H:C) and the oxygen-to-carbon (O:C) atomic ratios are commonly used for fuel characterization with respect to the thermochemical conversion. These ratios are illustrated with van Krevelen diagram presented in Fig. 6. High values of the H:C ratio correspond to the volatile-rich samples, such as biomass fuels in general and SCG in particular. During both treatments, the samples were shifting towards lower H:C and O:C ratios with the temperature increase. Volatilization and depolymerization during conversion processes reduced oxygen and increase carbon contents. At the same time, both torrefaction and HTC had a negligible effect on the samples during low-temperature tests due to limited devolatilization.

Thermogravimetric analysis

TGA results for SCG, Torre-300 and HTC-240 samples are presented in Fig. 7. The untreated SCG indicated slight initial mass loss between 50 to 200 °C under both air and N_2 atmospheres. This mass loss could be associated with moisture evaporation and release of very light volatiles. Such peak is lacking for both char samples in N_2, since pre-treatments already resulted in partial loss of the volatiles. The main degradation took place at temperatures between 200 and 500 °C with a maximum weight loss rate at 313 °C in N_2 and between 200 and 620 °C with a peak at 310 °C in air for SCG. The overlap of hemicellulose and cellulose decomposition results the shoulder around 380 °C in inert conditions (Pala et al., 2014). In oxidizing conditions, two main stages of thermal degradation can be identified besides the initial drying: an intensive and rapid release of volatile compounds followed by higher molecular weight compounds release and char oxidation (Miranda et al., 2011). Within the second stage, the maximum weight loss rate is indicated with the DTG peaks at the 498 °C, 540 °C and 575 °C for Torre-300, HTC-240 and SCG correspondingly.

From the obtained curves, it can be seen that the degradation behaviour of SCG changed significantly after torrefaction and HTC. The main degradation peaks were shifted towards higher temperatures in comparison with feedstock proving higher

thermal stability of obtained chars. The observed peaks are significantly smaller for chars due to lower volatiles content. Within N_2 atmosphere, there appears an additional peak at 349 °C before the main devolatilization peak at 407 °C in case of Torre-300. As for HTC-240, an additional shoulder at 276 °C before devolatilization peak around 376 °C can be identified. The percentages of the residual weight left after the TGA for char samples were almost identical: 29.9 wt% for Torre-300 and 33.2 wt% for HTC-240. Under oxidizing conditions, the thermal degradation occurred over a wider temperature range for hydrochar sample, which can be explained by degradation of repolymerization products remained after the HTC treatment (Pala et al., 2014).

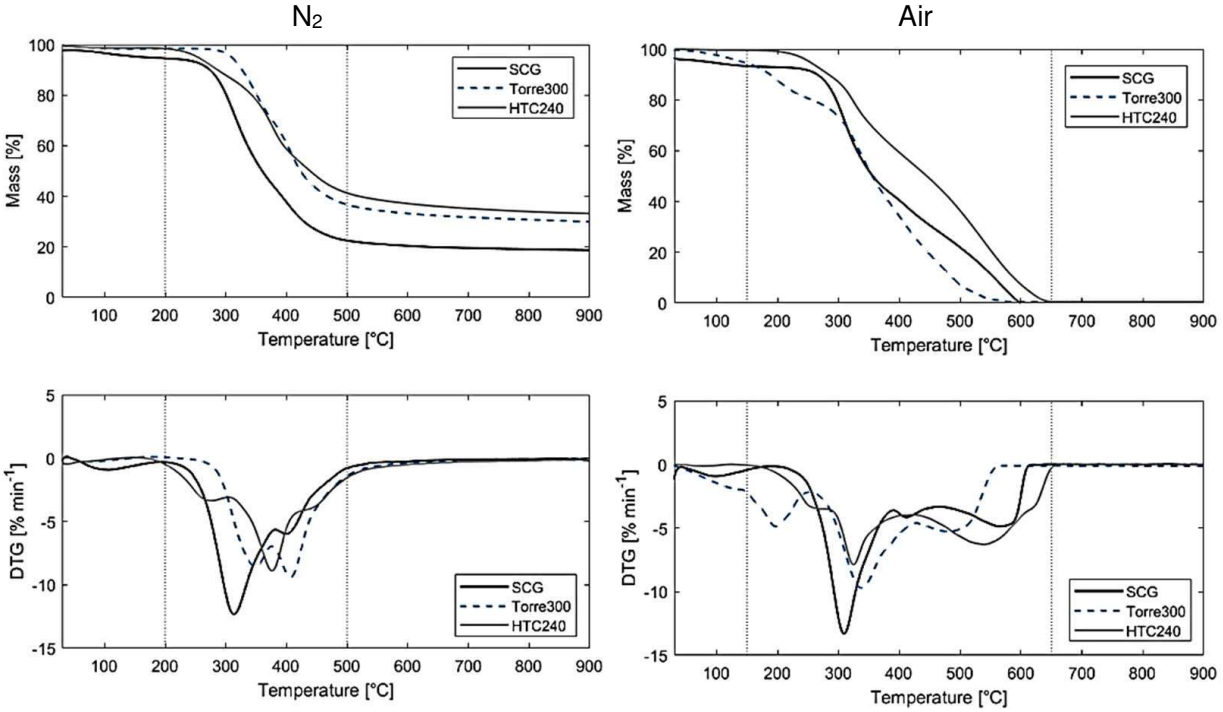

Figure 7. TG/DTG profiles of SCG and derived chars under nitrogen and air atmospheres.

Morphological structure analysis

The effect of torrefaction and HTC on the SCG morphology is illustrated with SEM images (Fig. 8). There were no visible changes between SCG and the char samples after low-temperature torrefaction, so the micrographs of Torre-260 and Torre-300 were chosen to show the effect of this conversion method. SCG prior the treatments exhibited a rough and irregular surface morphology, consistent with those reported in a previous studies (Yeung et al., 2014; Afolabi et al., 2020). While some porosity can be seen already for the feedstock sample, the increase of reaction temperature led to the considerable development of porous structures during both treatments. High-temperature experiments resulted in a major transformation of surface morphologies of the produced chars. The changes were associated with the reduction in organic compounds and devolatilization. The sample HTC-240 was significantly different from the others: high concentration of small particles of irregular shapes and dimensions. Furthermore, the obtained porosity was more structural in case of hydrochars than the torrefaction samples. The obtained results are consistent with the previously published findings, proving that the HTC leads to more intense

decomposition of feedstock (Kambo & Dutta, 2015; Babinszki et al., 2020) At higher temperatures, the hydrothermal conditions result not only the depolymerization and degradation of the primary biomass components, but in addition, the condensation of the reaction products from the liquid phase onto the hydrochar matrix as a secondary char (Lucian et al., 2018). A greater degree of polymerization via intermolecular dehydration reactions may be one possible explanation to smaller particle sizes of hydrochar obtained after HTC at 240 °C.

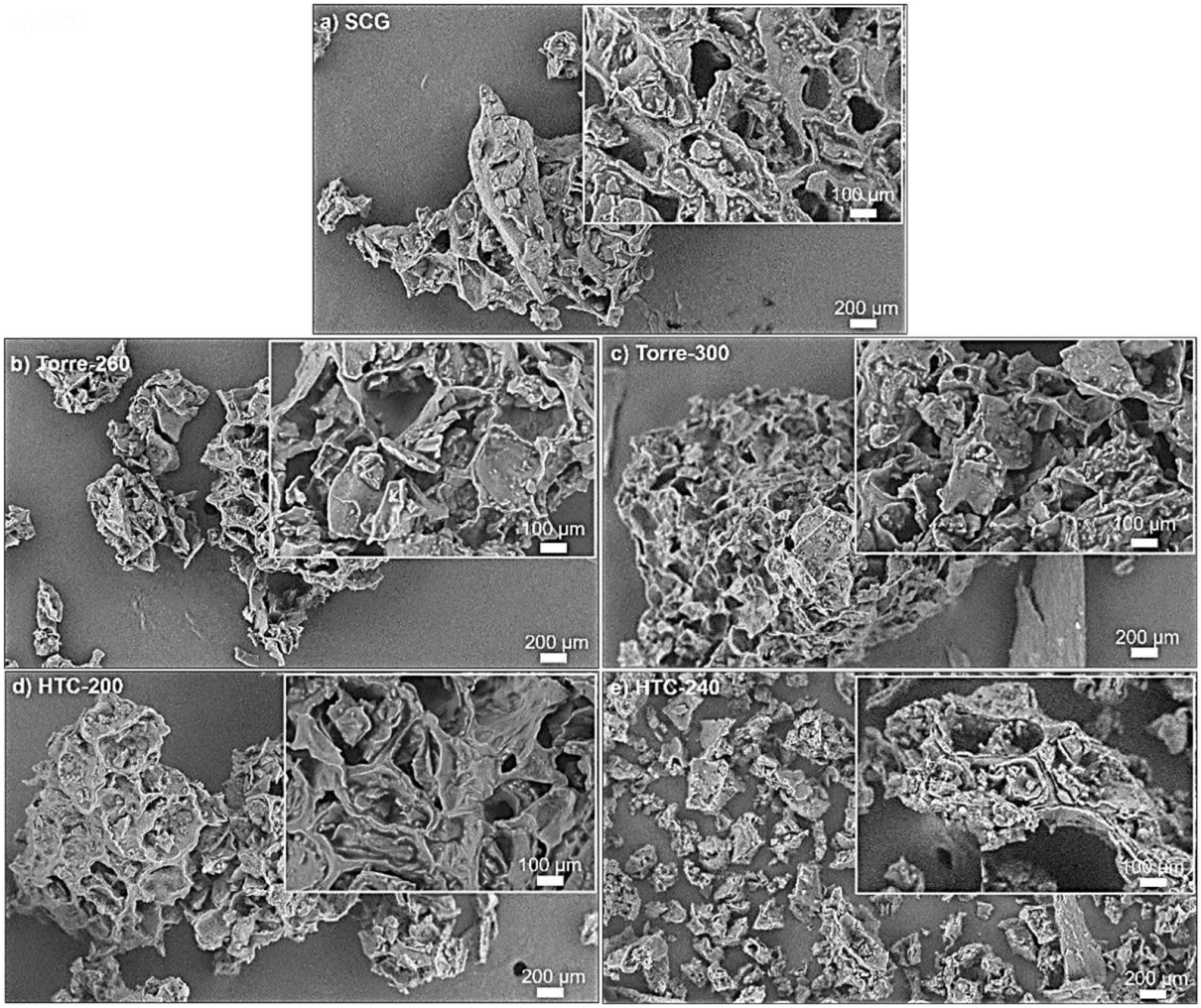

Figure 8. SEM images of spent coffee grounds and chars after torrefaction and HTC.

CONCLUSIONS

The current study investigated the effect of two thermal treatments methods, namely torrefaction and HTC, on the energy-related characteristics of spent coffee grounds. This valuable and currently underestimated feedstock has revealed a significant energy potential that can be improved even further with various thermal pre-treatment methods. The typical reaction temperatures of 200–300 °C for torrefaction and 200–240 °C for HTC were used. The feedstock decomposition intensified with temperature increase during both methods: char mass yield varied between 97.5% and 68.1% for torrefaction and 80.5% and 72.3% for HTC. Both processes resulted in a comparable relative increase of the heating value: 23% in the case of torrefaction at

300 °C and 29% in the case of HTC at 240 °C. The energy yield of HTC increased with temperature from 84.1% for HTC-200 to 93.0% for HTC-240. Alternatively, in the case of torrefaction, higher mass losses resulted in a descending trend for energy yield with temperature from 97.5% for Torre-200 to 84.1% for Torre-300. However, the energy yields for HTC and high-temperature torrefaction (> 250 °C) averaged over the temperature were 87.8% and 87.9% correspondingly. It means that both treatments had relatively similar energy conversion efficiencies.

The release of the volatile compounds and increase of the fixed carbon of SCG during both treatments intensified with temperature. The ash content of the chars produced with torrefaction grew from 1.13 wt% (SCG) to 1.89% (Torre-300). An opposite tendency was in the case of HTC: hydrothermal conditions led to the dissolving of ash forming minerals and ash content decreased to 0.19 wt% (HTC-240). As for the elemental composition, devolatilization and depolymerization reduced oxygen and increased carbon contents during both conversion processes. At the highest temperatures, produced chars indicated 23–28% more carbon and 43–46% less oxygen for torrefaction and HTC correspondingly. The untreated SCG sample was noticeably more reactive during TGA analysis in comparison with the tested char samples. The samples Torre-300 and HTC-240 were more stable under both inert and oxidizing conditions.

The obtained results confirmed that both hydrothermal carbonization and torrefaction could considerably increase the energy content of spent coffee grounds and convert it to highly carbonaceous char with increased energy content. Within the limits of selected reaction parameters, HTC showed slightly higher energy densification rates and more intensive decomposition of feedstock in comparison with torrefaction. An optimal selection of reaction settings affects the efficiency of the treatment and product characteristics. The overall efficiency of the process will be influenced by the heat supply method and subsequent utilization of the char and should be further investigated.

ACKNOWLEDGEMENTS. Authors highly appreciated the help of Toni Väkiparta, D.Sc., in making SEM images of the samples. Special thanks to Jussi Saari, D.Sc., for his valuable input of the coffee feedstock for the current experiments.

REFERENCES

Afolabi, O.O.D., Sohail, M. & Cheng, Y.L. 2020. Optimisation and characterisation of hydrochar production from spent coffee grounds by hydrothermal carbonisation. *Renew. Energy* **147**, 1380–1391. doi: 10.1016/j.renene.2019.09.098

Atabani, A.E., Mercimek, S.M., Arvindnarayan, S., Shobana, S., Kumar, G., Cadir, M. & Al-Muhatseb, A.H. 2018. Valorization of spent coffee grounds recycling as a potential alternative fuel resource in Turkey: An experimental study. *J. Air Waste Manag. Assoc.* **68**(3), 196–214. doi: 10.1080/10962247.2017.1367738

Babinszki, B., Jakab, E., Sebestyén, Z., Blazsó, M., Berényi,B., Kumar, J., Krishna, B.B., Bhaskar, T. & Czégény, Z. 2020. Comparison of hydrothermal carbonization and torrefaction of azolla biomass: Analysis of the solid products. *J. Anal. Appl. Pyrolysis* **149**, 104844. doi: 10.1016/j.jaap.2020.104844

Barbanera, M. & Muguerza, I.F. 2020. Effect of the temperature on the spent coffee grounds torrefaction process in a continuous pilot-scale reactor. *Fuel* **262**, 116493. doi: 10.1016/j.fuel.2019.116493

Broch, A., Jena, U., Hoekman, S.K. & Langford, J. 2014. Analysis of solid and aqueous phase products from hydrothermal carbonization of whole and lipid-extracted algae. *Energies* **7**(1), 62–79. doi: 10.3390/en7010062

Buratti, C., Barbanera, M., Lascaro, E. & Cotana, F. 2018. Optimization of torrefaction conditions of coffee industry residues using desirability function approach. *Waste Manag.* **73**, 523–534. doi: 10.1016/j.wasman.2017.04.012

Chen, W.H., Lin, B.J., Lin, Y.Y., Chu, Y.S., Ubando, A.T., Show, P.L., Ong, H.C., Chang, J.-S., Ho, S.-H., Culaba, A.B., Pétrissans, A. & Pétrissans, M. 2021. Progress in biomass torrefaction: Principles, applications and challenges. *Prog. Energy Combust. Sci.* **82**, 100887. doi: 10.1016/j.pecs.2020.100887

Choi, I.S., Wi, S.G., Kim, S.B. & Bae, H.J. 2012. Conversion of coffee residue waste into bioethanol with using popping pretreatment. *Bioresour. Technol.* **125**, 132–137. doi: 10.1016/j.biortech.2012.08.080

Donahue, C.J., & Rais, E.A. 2009. Proximate analysis of coal. *J. Chem. Educ*. **86**(2), 222–224. doi: 10.1021/ed086p222

Duman, G., Balmuk, G., Cay, H., Kantarli, I.C. & Yanik, J. 2020. Comparative Evaluation of Torrefaction and Hydrothermal Carbonization: Effect on Fuel Properties and Combustion Behavior of Agricultural Wastes. *Energy and Fuels* **34**(9), 11175–11185. doi: 10.1021/acs.energyfuels.0c02255

Felber, R., Hüppi, R., Leifeld, J. & Neftel, A. 2012. Nitrous oxide emission reduction in temperate biochar-amended soils. *Biogeosciences Discuss.* **9**(1), 151–189. doi: 10.5194/bgd-9-151-2012

Fornes, F., Belda, R.M., Fernández de Córdova, P. & Cebolla-Cornejo, J. 2017. Assessment of biochar and hydrochar as minor to major constituents of growing media for containerized tomato production. *J. Sci. Food Agric.* **97**(11), 3675–3684. doi: 10.1002/jsfa.8227

Fuente-Hernández, A., Lee, R., Béland, N., Zamboni, I. & Lavoie, J.M. 2017. Reduction of furfural to furfuryl alcohol in liquid phase over a biochar-supported platinum catalyst. *Energies* **10**(3). doi: 10.3390/en10030286

Funke, A. & Ziegler, F. 2010. Hydrothermal carbonization of biomass: A summary and discussion of chemical mechanisms for process engineering. *Biofuels, Bioprod. Biorefining* **4**(2), 160–177. doi: 10.1002/bbb.198

Haile, M., Asfaw, A. & Asfaw, N. 2013. Investigation of waste coffee ground as a potential raw material for biodiesel production. *Int. J. Renew. Energy Res.* **3**(4), 854–860. doi: 10.20508/ijrer.23113

ICO. 2020. International Coffee Organization - What's New. http://www.ico.org/ (accessed 4 September 2020).

Kambo, H.S & Dutta, A. 2014. Strength, storage, and combustion characteristics of densified lignocellulosic biomass produced via torrefaction and hydrothermal carbonization. *Appl. Energy* **135**: 182–191. doi: 10.1016/j.apenergy.2014.08.094

Kambo, H.S. & Dutta, A. 2015. Comparative evaluation of torrefaction and hydrothermal carbonization of lignocellulosic biomass for the production of solid biofuel. *Energy Convers. Manag.* **105**, 746–755. doi: 10.1016/j.enconman.2015.08.031

Kante, K., Nieto-Delgado, C., Rangel-Mendez, J.R. & Bandosz, T.J. 2012. Spent coffee-based activated carbon: Specific surface features and their importance for H 2S separation process. *J. Hazard. Mater.* **201–202**, 141–147. doi: 10.1016/j.jhazmat.2011.11.053

Kasongo, R.K., Verdoodt, A., Kanyankagote, P., Baert, G. & Ranst, E.V. 2011. Coffee waste as an alternative fertilizer with soil improving properties for sandy soils in humid tropical environments. *Soil Use Manag.* **27**(1), 94–102. doi: 10.1111/j.1475-2743.2010.00315.x

Kim, D., Lee, K., Bae, D. & Park, K.Y. 2017. Characterizations of biochar from hydrothermal carbonization of exhausted coffee residue. *J. Mater. Cycles Waste Manag.* **19**(3), 1036–1043. doi: 10.1007/s10163-016-0572-2

Kwon, E.E., Yi, H. & Jeon, Y.J. 2013. Sequential co-production of biodiesel and bioethanol with spent coffee grounds. *Bioresour. Technol.* **136**, 475–480. doi: 10.1016/j.biortech.2013.03.052

Libra, J.A., Ro, K.S., Kammann, C., Funke, A., Berge, N.D., Neubauer, Y., Titirici, M.M., Fühner, C., Bens, O., Kern, J. & Emmerich, K.H. 2011. Hydrothermal carbonization of biomass residuals: A comparative review of the chemistry, processes and applications of wet and dry pyrolysis. *Biofuels* **2**(1), 71–106. doi: 10.4155/bfs.10.81

Liu, Z. & Balasubramanian, R. 2014. Upgrading of waste biomass by hydrothermal carbonization (HTC) and low temperature pyrolysis (LTP): A comparative evaluation. *Appl. Energy* **114**, 857–864. doi: 10.1016/j.apenergy.2013.06.027

Lucian, M., Volpe, M., Gao, L., Piro, G., Goldfarb, J.L. & Fiori, L. 2018. Impact of hydrothermal carbonization conditions on the formation of hydrochars and secondary chars from the organic fraction of municipal solid waste. *Fuel* **233**, 257–268. doi: 10.1016/j.fuel.2018.06.060

Massaya, J., Chan, K.H., Mills-Lamptey, B. & Chuck, C.J. 2021. Developing a biorefinery from spent coffee grounds using subcritical water and hydrothermal carbonisation. *Biomass Convers. Biorefinery* **1–17**. doi: 10.1007/s13399-020-01231-w

Miranda, M.T., Arranz, J.I., Román, S., Rojas, S., Montero, I., López, M. & Cruz, J.A. 2011. Characterization of grape pomace and pyrenean oak pellets. *Fuel Processing Technology*. Elsevier. p. 278–283.

Moustafa, H., Guizani, C., Dupont, C., Martin, V., Jeguirim, M. & Dufresne, A. 2017. Utilization of torrefied coffee grounds as reinforcing agent to produce high-quality biodegradable PBAT composites for food packaging applications. *ACS Sustain. Chem. Eng.* **5**(2), 1906–1916. doi: 10.1021/acssuschemeng.6b02633

Murthy, P.S. & Naidu, M.M. 2012. Recovery of Phenolic Antioxidants and Functional Compounds from Coffee Industry By-Products. *Food Bioprocess Technol.* **5**(3), 897–903. doi: 10.1007/s11947-010-0363-z

Nizamuddin, S., Baloch, H.A., Siddiqui, M.T.H., Mubarak, N.M., Tunio, M.M., Bhutto, A.W. & Srinivasan, M.P. 2018. An overview of microwave hydrothermal carbonization and microwave pyrolysis of biomass. *Rev. Environ. Sci. Biotechnol.* **17**(4), 813–837. doi: 10.1007/s11157-018-9476-z

Pala, M., Kantarli, I.C., Buyukisik, H.B. & Yanik, J. 2014. Hydrothermal carbonization and torrefaction of grape pomace: A comparative evaluation. *Bioresour. Technol.* **161**, 255–262. doi: 10.1016/j.biortech.2014.03.052

Paneque, M., De la Rosa, J.M., Kern, J., Reza, M.T. & Knicker, H. 2017. Hydrothermal carbonization and pyrolysis of sewage sludges: What happen to carbon and nitrogen? *J. Anal. Appl. Pyrolysis* **128**, 314–323. doi: 10.1016/j.jaap.2017.09.019

Partridge, A., Sermyagina, E. & Vakkilainen, E. 2020. Impact of pretreatment on hydrothermally carbonized spruce. *Energies* **13**(11). doi: 10.3390/en13112984

Reed, T.B. & Gaur, S. 1994. Atlas of thermal data of biomass and other fuels-a report on the forthcoming book. Pergamon.

Rodriguez Correa, C., Hehr, T., Voglhuber-Slavinsky, A., Rauscher, Y. & Kruse, A. 2019. Pyrolysis vs. hydrothermal carbonization: Understanding the effect of biomass structural components and inorganic compounds on the char properties. *J. Anal. Appl. Pyrolysis* **140**, 137–147. doi: 10.1016/j.jaap.2019.03.007

Román, S., Nabais, J.M.V, Laginhas, C., Ledesma, B. & González, J.F. 2012. Hydrothermal carbonization as an effective way of densifying the energy content of biomass. *Fuel Process.* Technol. **103**, 78–83. doi: 10.1016/j.fuproc.2011.11.009

Sermyagina, E., Saari, J., Kaikko, J. & Vakkilainen, E. 2015. Hydrothermal carbonization of coniferous biomass: Effect of process parameters on mass and energy yields. *J. Anal. Appl. Pyrolysis* **113**, 551–556. doi: 10.1016/j.jaap.2015.03.012

Sermyagina, E., Murashko, K., Nevstrueva, D. & Vakkilainen, E. 2020. Conversion of cellulose to activated carbons for high-performance supercapacitors. *Agron. Res.* **18**(3), 2197–2210. doi: 10.15159/AR.20.163

SFS, 2009a. EN 14774-2 Solid biofuels - Determination of moisture content - Oven dry method - Part 2: Total moisture - Simplified method.

SFS, 2009b. SFS-EN 14775:en Solid biofuels. Determination of ash content.

SFS, 2012. EN 15148 Solid biofuels - Determination of the content of volatile matter.

SFS, 2015. ISO 16948 Solid biofuels. Determination of total content of carbon, hydrogen and nitrogen.

SFS, 2016. ISO 16994 Solid biofuels. Determination of total content of sulfur and chlorine.

Tamelová, B., Malaťák, J. & Velebil, J. 2019. Hydrothermal carbonization and torrefaction of cabbage waste. *Agron. Res.* **17**(3), 862–871. doi: 10.15159/AR.19.098

Urbancl, D., Krope, J. & Goričanec, D. 2019. Torrefaction-the process for biofuels production by using different biomasses. *Agron. Res.* **17**(4), 1800–1807. doi: 10.15159/AR.19.176.

Velebil, J. 2018. Energy valorisation of citrus peel waste by torrefaction treatment. *Agron. Res*. **16**(1), 276. doi: 10.15159/AR.18.029

Vítězová, M., Jančiková, S., Dordević, D., Vítěz, T., Elbl, J., Hanišáková, N., Jampílek, J. & Kushkevych, I. 2019. The Possibility of Using Spent Coffee Grounds to Improve Wastewater Treatment Due to Respiration Activity of Microorganisms. *Appl. Sci.* **9**(15), 3155. doi: 10.3390/app9153155

Yamane, K., Kono, M., Fukunaga, T., Iwai, K., Sekine, R., Watanabe, Y. & Iijima, M. 2014. Field evaluation of coffee grounds application for crop growth enhancement, weed control, and soil improvement. *Plant Prod. Sci.* **17**(1), 93–102. doi: 10.1626/pps.17.93

Yen, W.J., Wang, B.S., Chang, L.W. & Duh, P.D. 2005. Antioxidant properties of roasted coffee residues. *J. Agric. Food Chem*. doi: 10.1021/jf0402429

Yeung, P.T., Chung, P.Y., Tsang, H.C., Cheuk-On Tang, J., Yin-Ming Cheng, G., Gambari, R. & Lam, K.H. 2014. Preparation and characterization of bio-safe activated charcoal derived from coffee waste residue and its application for removal of lead and copper ions. *RSC Adv*. **4**(73), 38839–38847. doi: 10.1039/c4ra05082g

Zhang, C., Ho, S.H., Chen, W.H., Xie, Y., Liu, Z. & Chang, J.S. 2018. Torrefaction performance and energy usage of biomass wastes and their correlations with torrefaction severity index. *Appl. Energy* **220**, 598–604. doi: 10.1016/j.apenergy.2018.03.129

Zhuang, X., Zhan, H., Song, Y., He, C., Huang, Y., Yin, X. & Wu, C. 2019. Insights into the evolution of chemical structures in lignocellulose and non-lignocellulose biowastes during hydrothermal carbonization (HTC). *Fuel* **236**, 960–974. doi: 10.1016/j.fuel.2018.09.019